

Photoionization of Atomic Chlorine

B. Rušćić^(a) and J. Berkowitz

Argonne National Laboratory, Argonne, Illinois 60439

(Received 28 December 1982)

The experimental ion-yield curve for photoionization of atomic chlorine from the ionization threshold ($\sim 956.1 \text{ \AA}$) to 750 \AA is reported. Three autoionizing series converging to the 1D_2 ionic state and two series converging to the 1S_0 state are observed. The results are compared to existing many-body calculations.

PACS numbers: 32.80.Fb, 32.70.Jz, 32.80.Dz, 35.10.Hn

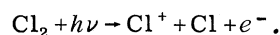
The photoionization spectra of most atoms and diatomics, in the first few electronvolts above the ionization threshold, are replete with resonance structure due to the process called autoionization. One way of describing the underlying physics is through discrete-state-continuum interaction, which in most instances involves electron-electron interaction. Most *ab initio* theories of photoionization,¹ being essentially single-electron theories, focus on the nonresonant processes. Several types of many-body theories (MBT) which incorporate the autoionization resonances are currently being developed. One, which has proved successful in reproducing these resonances in the noble gases, begins with an *ab initio* calculation using the relativistic random-phase approximation (RRPA).² From this, dynamical parameters are obtained for calculating the energy positions and peak profiles of the resonances through a multichannel quantum-defect theory (MQDT). This theory has not yet been adapted to open-shell atoms. However, two other theories, *R*-matrix³ and diagrammatic MBT,⁴ have attempted to describe autoionization resonances in atomic chlorine. In order to test these theories, and to provide a guide for future calculations, we have measured the relative photoionization cross section of atomic chlorine from the ionization threshold to 750 \AA .

Experimental arrangement.—Atomic chlorine was prepared in a microwave discharge through pure Cl_2 at ~ 0.5 Torr in a quartz tube with metaphosphoric acid coating. The products traversed a distance of ~ 35 cm, in a fast-flow system, past a 0.5 -mm-diam orifice and then on to a liquid-nitrogen trap. Species effusing through the orifice entered a photoionization region situated circa 1 cm beyond.

Radiation from the He Hopfield continuum was dispersed by a 3 -m vacuum ultraviolet monochromator. The selected wavelengths traversed the photoionization region, whereupon their inten-

sities were measured by a bare photomultiplier. Photoions were focused onto the entrance orifice of a quadrupole mass filter and detected by another bare multiplier, using pulse-counting techniques.

Experimental results.—The ion-yield curve for photoionization of atomic chlorine, obtained at a photon resolution of 0.28 \AA , and corrected for the wavelength dependence of the light detector's efficiency, is displayed in Fig. 1. The wavelength scale is calibrated against known impurity lines in the light spectrum and should be accurate to 0.1 \AA . The spectrum has been obtained in overlapping sections and patched together. In order to minimize cumulative error in relative intensity, a rapid scan of the whole spectrum was taken and the shorter segments matched to it. Below $\sim 802.7 \text{ \AA}$ the observed ion-yield curve contained an extraneous contribution from the photodissociative ionization^{5,6} of the residual Cl_2 :



To obtain the ion-yield curve due solely to atomic Cl, the yield of Cl^+ from Cl_2 between 750 and 810 \AA was subtracted, taking into account the ion intensities of Cl^+ and Cl_2^+ with discharge on and off. Four different calculations, including RPA,⁷ *R* matrix,³ diagrammatic MBT,⁴ and close coupling,⁸ agree to within a few percent on the absolute cross section in the *continuum* just beyond the 1S_0 threshold. We have normalized our relative ion-yield curve in this photon energy range to the average of these calculations (40.2 Mb), thus placing the intensity on an absolute scale, at least tentatively, within an estimated combined error of $\sim 20\%$.

A simple interpretation for the value of the ionization threshold is obscured by the presence of an autoionization peak (Fig. 1). Within this uncertainty, the threshold value of 956.35 \AA agrees with the previously established⁶ convergence limit (956.13 \AA) to 3P_2 . No evidence was found for

photoionization of excited Cl (${}^2P_{1/2}$). A few members of an autoionizing series converging to the 3P_1 state can be discerned. Any possible series converging upon the 3P_0 state were too weak to be observable above experimental scatter.

Three distinct series converging to the 1D_2 state are readily apparent. One has a broad, "anomalous" line profile. The other two are very narrow, their widths being limited by the instrumental resolution. All three series are clearly seen in the absorption spectrogram of Huffman, Larrabee, and Tanaka.⁶ The broad-series members have been fitted to the Fano line-profile formula.⁹ The values obtained for the line-profile index q and spectral width Γ are listed in Table I, together with the effective quantum numbers n^* obtained from the Rydberg formula. Within the experimental error, the convergence limit to 1D_2 is in good agreement with the previous measurements.⁶ The values of the quantum defects δ ($n^* = n - \delta$, n being the principal quantum number) and the quantity d ($d = |[n^* + 0.5] - n^*|$, where brackets denote the integer part), together with the widths Γ , are strongly reminiscent of previous observations in the noble gases¹⁰ and in atomic iodine and tellurium.¹¹

The broad series has $d \sim 0.3$, and can be associated with an antecedent below the ionization threshold at $101\,945.20\text{ cm}^{-1}$ assigned¹² as $3p^4({}^1D)3d, {}^2P_{1/2}$ or ${}^2P_{3/2}$. A plausible inference is that the broad series involves $p - nd$ excitations, resulting in quasidiscrete 2P states. The longer-wavelength narrow series has $d \sim 0.1$ and can be associated with two pairs of antecedents,¹² one at

TABLE I. Effective quantum numbers n^* and fitted parameters q and Γ for the three series converging to $3p^4({}^1D_2)$.

Rydberg term	n^*	q	Γ (cm^{-1})
$({}^1D)4d\ {}^2P$	3.716	1.54	715.2
$({}^1D)5d\ {}^2P$	4.692	1.52	406.8
$({}^1D)6d\ {}^2P$	5.680	1.54	239.0
$({}^1D)6s\ {}^2D$	3.898		
$({}^1D)7s\ {}^2D$	4.899		
$({}^1D)8s\ {}^2D$	5.908		
$({}^1D)9s\ {}^2D$	6.875		
$({}^1D)4d'\ {}^2D$	4.038		
$({}^1D)5d'\ {}^2D$	5.031		
$({}^1D)6d'\ {}^2D$	6.026		
$({}^1D)7d'\ {}^2D$	6.997		
$({}^1D)8d'\ {}^2D$	8.005		

$103\,101$ and $103\,102\text{ cm}^{-1}$, assigned as $3p^4({}^1D)5s\ {}^2D_{5/2,3/2}$ and another at $84\,120$ and $84\,122\text{ cm}^{-1}$ assigned as $3p^4({}^1D)4s\ {}^2D_{5/2,3/2}$. This series is therefore labeled in Fig. 1 as ns , and is to be associated with ${}^2D_{5/2,3/2}$ resonant states.

The coupling of a 1D_2 core with a "d" Rydberg electron can also give rise to ${}^2D_{5/2,3/2}$ and ${}^2S_{1/2}$ states. The latter, although having an identified member¹² below the ionization threshold ($99\,534.419\text{ cm}^{-1}$), should be unobservable in the photoionization spectrum because the 3P ionization continuum does not contain a ${}^2S_{1/2}$ channel, and hence autoionization is forbidden by selection rules.¹³ In fact, the predicted position of $3p^4({}^1D)4d\ {}^2S_{1/2}$ is at $929\text{--}932\text{ \AA}$, corresponding to a deep valley in the photoionization spectrum. Thus, the other narrow series, more intense and to shorter wavelength, with $d \sim 0.03$, has to be associated with the remaining $nd\ {}^2D_{5/2,3/2}$ resonant states. Its nearest antecedent would be predicted to occur at $\sim 104\,300\text{ cm}^{-1}$, which is below the ionization threshold but in a region not well explored.¹² A state at $102\,187.51\text{ cm}^{-1}$ has been tentatively assigned¹² as $3p^4({}^1D)3d\ {}^2D_{5/2}$, although a transition from the ground state to this state has not been observed. Acceptance of such an assignment would give a noncongruent quantum defect for the antecedent, and the order of the two narrow series would reverse upon crossing the ionization threshold. A more detailed analysis which includes mixing of the resonance states of the same symmetry is currently in progress.

Finally, two series can be seen converging to the 1S_0 ionic state. Their d values are close, but their relative intensity and shape change with increasing quantum number. The effective quantum numbers, listed in Table II, are based on a limit of $132\,420\text{ cm}^{-1}$, which yields more constant quantum defects in both series than the limit $132\,467\text{ cm}^{-1}$ given by Huffman, Larrabee, and Tanaka.⁶ The series to higher energy, with $d \approx 0.12\text{--}0.13$, has an identifiable antecedent in the discrete spectrum at $101\,596.44\text{ cm}^{-1}$, assigned¹² to the state $3p^4({}^1S)4s\ {}^2S_{1/2}$, and is therefore labeled as an ns series in Fig. 1. The other series has $d \approx 0.25\text{--}0.3$. This nd series has no apparent antecedents, because the first member already corresponds to the $3p^4({}^1S)3d\ {}^2D_{5/2,3/2}$ resonant state.

Discussion and comparison with calculations.

—We first consider the resonances converging to 1D_2 . In the R -matrix calculations, only the $3p^4({}^1D)nd\ {}^2P$ series has been reported.³ Our fitted line shapes give an almost constant profile index

TABLE II. Effective quantum numbers n^* for the two series converging to $3p^4(^1S_0)$ with the adjusted limit of $132\,420\text{ cm}^{-1}$.

Rydberg term	n^*
$(^1S)3d\ ^2D$	2.807
$(^1S)4d\ ^2D$	3.746
$(^1S)5d\ ^2D$	4.722
$(^1S)6d\ ^2D$	5.706
$(^1S)7d\ ^2D$	6.713
$(^1S)8d\ ^2D$	7.721
$(^1S)9d\ ^2D$	8.759
$(^1S)10d\ ^2D$	9.746
$(^1S)5s\ ^2S$	2.876
$(^1S)6s\ ^2S$	3.880
$(^1S)7s\ ^2S$	4.883
$(^1S)8s\ ^2S$	5.880
$(^1S)9s\ ^2S$	6.870

q for $n=4, 5$, and 6 . Lamoureux and Combet-Farnoux³ report the fitted parameters only for $n=7$ ($q=2.73$) and $n=8$ ($q=2.65$). We have extrapolated our fitted widths to higher series members, using the criterion $(n^*)^3\Gamma \approx \text{const}$. These Γ 's are about 1.7 times larger than the calculated values based on a case-II, or configuration-

interaction (CI) calculation, although their case-I calculation (no CI) gives a broader resonance. Our quantum defects span the range $0.285-0.32$ and the antecedent discrete state has $\delta=0.23$. The R -matrix calculations give $\delta=0.164, 0.168$ for $n=7, 8$ and $\delta=0.03$ for the discrete state. The calculated resonances display a weaker interaction with the continuum, giving rise to larger q values and smaller Γ values. The maximum of the calculated resonance differs from the experimental value by almost a factor 3, at least partly because of a significant underestimate of the continuum cross section in this region.

Both nd and ns resonances have been treated in the diagrammatic MBT calculations,⁴ and they encompass the 2D and 2P channels. The 2P channel corresponds to our broad series. The authors⁴ have not provided fitted parameters, making a detailed comparison difficult, although the shape, the estimated quantum defects, and the cross sections at the peaks and valleys of the 2P resonances seem to be in rather good agreement with the experimental values.

Brown, Carter, and Kelly⁴ used their coupled-equations code to generate "the sum of the $^1Dns-^2D$ and $^1Dnd^2D$ resonances," resulting in a single series of sharp peaks with associated sharp val-

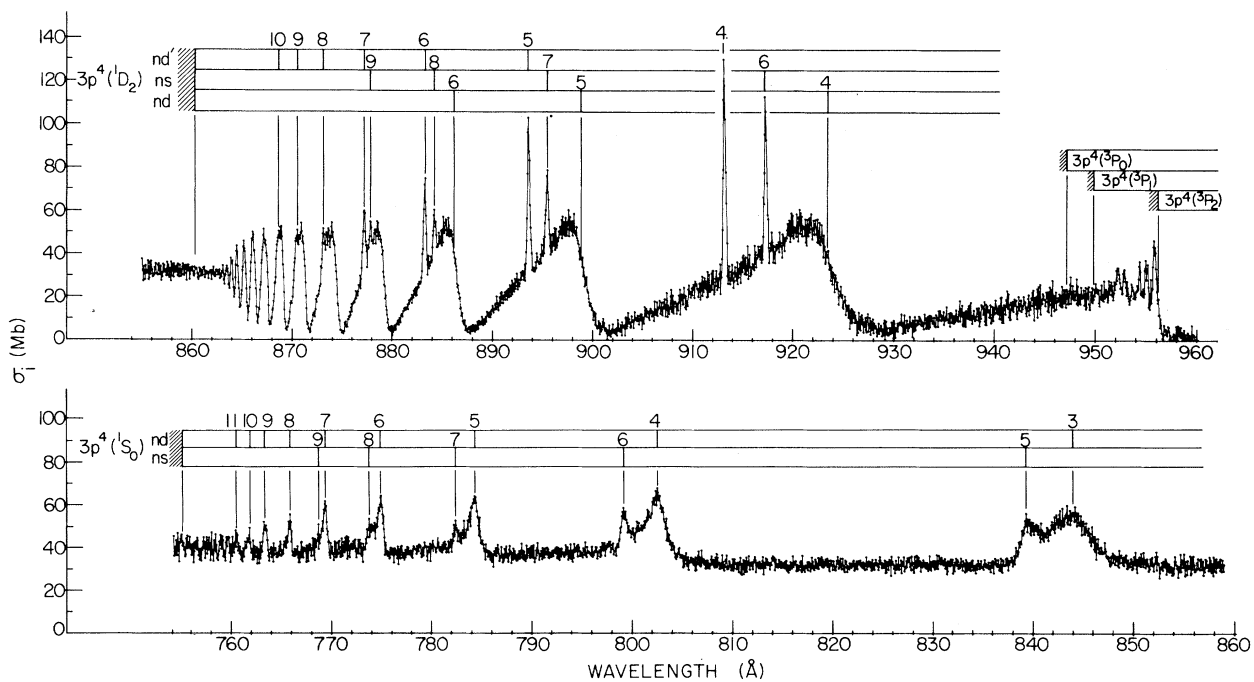


FIG. 1. Photoionization-yield curve of atomic chlorine. Optical resolution is 0.28 \AA (full width at half maximum). Three series of resonances (one broad, two narrow) converging to $\text{Cl}^+, 3p^4(^1D_2)$ are observed and assigned, and two series can be seen converging to $\text{Cl}^+, 3p^4(^1S_0)$. Absolute cross section σ_i is tentative, based on concordance of several theoretical calculations in the continuum beyond the 1S_0 limit.

leys penetrating into the broad 2P resonances. In the experimental spectrum, two series of sharp peaks result, presumably from the same interacting 2D series. From Fig. 11 of Ref. 4, we estimate $n^* = 4.03$ and 4.91 for the first two sharp members. These numbers suggest an interplay between the two 2D series, since the first member has an effective quantum number very close to our labeled " nd " series, while the latter corresponds closely to our labeled " ns " series.

Next we turn to the resonances converging to 1S_0 . In the R -matrix calculations, only the $3p^4$ -(1D) nd^2D series has been treated.³ The reported quantum defects are much too low in both case II and case I. In case II the resonances appear too narrow by almost a factor of 2 and the peak values are correspondingly too high. The shape of the resonances in case I appears to conform more closely to experiment. The continuum cross section is again greatly underestimated here.

The sum of the (1S) ns^2S and (1S) nd^2D channels is reported in the diagrammatic MBT calculations,⁴ superposed on the nonresonant background. A broader d resonance precedes a narrower s resonance in energy, in agreement with experiment. The quantum defects deduced from Fig. 12 of Ref. 4 for both nd and ns series compare favorably to the experimental values, as well as the calculated absolute intensities of resonant and nonresonant portions of the spectrum. The main discrepancy occurs in the first resonance, which displays unresolved s and d components in the calculation, whereas they are resolved in the spectrum.

In summary, the diagrammatic MBT calculation provides a fairly good representation of the experimental spectrum, much better in several

respects than the R -matrix calculation. The major discrepancy between diagrammatic MBT and experiment is the appearance of a single sharp ns series converging to 1D , and accompanied by a dip, whereas the experimental spectrum displays two narrow series. Further experimental work is in progress. A more detailed analysis of the experimental spectrum will be provided in the near future.

This research was supported by the U. S. Department of Energy, Office of Basic Energy Sciences, under Contract No. W-31-109-Eng-38.

(a)On leave from "Ruger Bošković" Institute, Zagreb, Yugoslavia.

¹See, for example, S. T. Manson, A. Msezane, A. F. Starace, and S. Shahabi, *Phys. Rev. A* **20**, 1005 (1979).

²W. R. Johnson, K. T. Cheng, K.-N. Huang, and M. LeDourneuf, *Phys. Rev. A* **22**, 989 (1980).

³M. Lamoureux and F. Combet-Farnoux, *J. Phys. Paris* **40**, 545 (1979).

⁴E. R. Brown, S. L. Carter, and H. P. Kelly, *Phys. Rev. A* **21**, 1237 (1980).

⁵K. P. Huber and G. Herzberg, *Molecular Spectra and Molecular Structure. IV. Constants of Diatomic Molecules* (Van Nostrand Reinhold, New York, 1979).

⁶R. E. Huffman, J. C. Larrabee, and Y. Tanaka, *J. Chem. Phys.* **47**, 856 (1967), and **48**, 3835 (1968).

⁷N. A. Cherepkov and L. V. Chernysheva, *Phys. Lett.* **60A**, 103 (1977).

⁸M. J. Conneely, Ph.D. thesis, London University, 1969 (unpublished).

⁹U. Fano, *Phys. Rev.* **124**, 1866 (1961).

¹⁰K. Radler and J. Berkowitz, *J. Chem. Phys.* **70**, 216 (1979).

¹¹J. Berkowitz, C. H. Batson, and G. L. Goodman, *Phys. Rev. A* **24**, 149 (1981).

¹²L. J. Radziemski, Jr., and V. Kaufman, *J. Opt. Soc. Am.* **59**, 424 (1981).

¹³See, for example, G. Herzberg, *Atomic Spectra and Atomic Structure* (Dover, New York, 1944), p. 173.